JOURNAL OF SOLID STATE CHEMISTRY 120, 320–326 (1995)

Synthesis of Vanadium Carbide by Temperature Programmed Reaction

Rajat Kapoor and S. T. Oyama

Department of Chemical Engineering, Virginia Polytechnic Institute and State University, Blacksburg, Virginia 24061-0211

Received January 18, 1995; received July 27, 1995; accepted August 1, 1995

Vanadium carbide powders are prepared with moderate surface areas of 60 $m^2 g^{-1}$ (particle size 17 nm) by a temperature programmed reaction between solid vanadium pentoxide (19 $m^2 g^{-1}$) and a methane–hydrogen mixture. The synthesis involves two steps. In the first step a single suboxide intermediate, V_2O_3, is formed by reduction of V_2O_5 by hydrogen at 800 K. In the second step the V_2O_3 is reduced and carburized by methane with production of CO at 1180 K. In the early stages, the synthesis is found to be limited by the activation of hydrogen as found from experiments with Pt/V_2O_5. The transformation is accompanied by retention of external shape and size, and so is pseudomorphic, but does not conserve orientation of crystallographic planes, so is not topotactic. The results are compared and contrasted to those of nitridation with ammonia and reduction by pure hydrogen. © 1995 Academic Press, Inc.

INTRODUCTION

The early transition metal carbides form an interesting group of materials that have properties suitable for application in diverse fields such as metallurgy (1), electronics (2), and catalysis (3). Unlike the traditional applications in metallurgy, the use of these materials in catalysis requires them to possess high specific surface areas (S_g). Considerable research has been done in the preparation of these catalytically active carbides (3), and of the various methods employed, the temperature programmed synthesis method (4) using oxide precursors has shown potential for producing high S_g materials in large quantities. The subject of this paper is the study of vanadium carbide synthesis from vanadium pentoxide using temperature programmed techniques.

In this study, the intermediate phases were identified and the development of surface area was studied. The occurrence of topotactic and pseudomorphic phenomena for the oxide to carbide transformation was investigated, and its significance is discussed. The results of the synthesis and characterization were compared with our earlier work on the synthesis of vanadium nitrides (5, 6). Hydrogen activation limitation in these syntheses was studied using platinum on vanadia as a precursor.

EXPERIMENTAL

Vanadium carbide powders were prepared by using a temperature programmed reaction (TPR) technique where vanadium pentoxide was reduced to a V_2O_3 suboxide and finally carburized by a 20% mixture of CH_4/H_2 (7) gas. A typical run consisted of loading 400 mg (2200 μmol) of V_2O_5 into a microreactor, establishing a 400 $cm^3 min^{-1}$ (270 $\mu mol\ s^{-1}$) flow of the carburizing mixture (space velocity = 67,000 h^{-1}) and heating the sample according to the temperature program. The temperature was raised in two stages, first rapidly to 430 K, and then slowly to a final synthesis temperature, T_f. The linear heating rates employed in the second stage varied from 0.03 to 0.2 K s^{-1} with T_f ranging from 1250 to 1320 K. The effluent gases were monitored by an on-line mass spectrometer and the signal for various species were collected and displayed in real-time with temperature. The variation in the signal allowed determination of intermediate stages and the end of reaction. After synthesis the product was cooled to room temperature in He and was passivated by a 0.5% O_2/He mixture. After the synthesis, the sample was characterized by N_2 BET, CO chemisorption, and X-ray powder diffraction (XRD).

In separate experiments, preferentially oriented V_2O_5 crystals were reduced and carburized under identical conditions. The preparation of the crystals was described in a previous publication (8). Additionally, these well-defined crystals were also reduced in pure H_2 under the same conditions. The products from both were analyzed by XRD and scanning electron microscopy (SEM). These measurements were carried out to study topotacticity and pseudomorphicity in the oxide to carbide transformation, as will be described later.

Since noble metals like platinum are known to activate H_2 at low temperatures, one of the carburization experiments was run using a finely dispersed platinum on vana-

0022-4596/95 $12.00

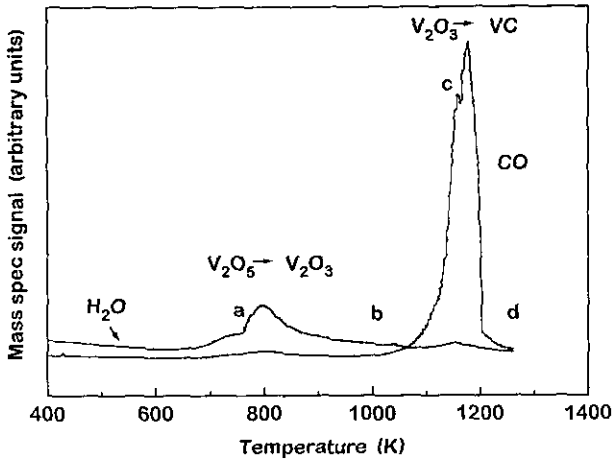

FIG. 1. VC synthesis by TPR; mass spectrometry signal for H_2O and CO vs temperature showing the progress of the reaction; SV = 67,000 h^{-1}, β = 0.03 K s^{-1}.

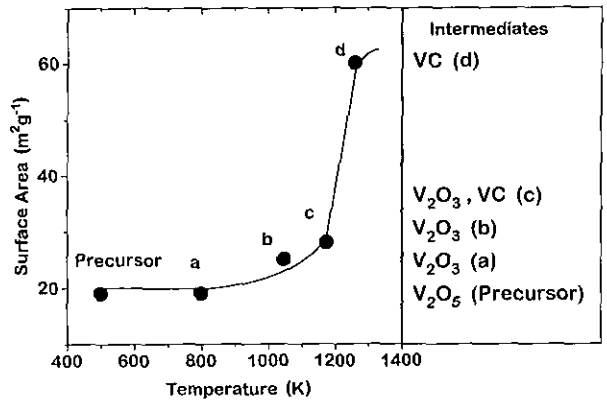

FIG. 3. The development of surface area during VC synthesis and intermediate phases.

dium oxide sample as the precursor. The sample was prepared by impregnating a solution of $H_2PtCl_6 \cdot 6H_2O$ on V_2O_5 to incipient wetness and calcining the solid in air. The sample thus prepared had a nominal concentration of 0.6 wt% Pt. The heating was carried out in two stages: In the first, the temperature was raised to 393 K (0.03 K s^{-1}) and maintained for 2 h. In the second, the temperature was raised to 673 K (0.083 K s^{-1}) and maintained for 4 hr.

RESULTS

The temperature programmed synthesis of VC was followed by monitoring masses 2 (H_2), 16 (CH_4), 18 (H_2O), 28 (CO), and 44 (CO_2). Figure 1 shows the traces of masses 18 (H_2O) and 28 (CO) versus temperature for the heating rate, β = 0.03 K s^{-1}. The H_2O trace shows a peak at 800 K with a shoulder at 760 K and a smaller peak at 1154 K. The CO trace shows a small peak at 793 K and a large peak at 1180 K. The CO_2 trace (not shown) was very weak and had two peaks centered below the CO peaks. The traces of H_2 and CH_4 were relatively featureless due to a large background signal and are not shown here. The end of the synthesis was marked by the return of the CO (second peak) signal to the baseline.

Four intermediate points were identified, shown in Fig. 1 as *a*, *b*, *c*, and *d*, corresponding to different stages of reaction. The synthesis was repeated under the same conditions and stopped at each of these points to determine the development of surface areas by N_2 BET measurements and the presence of intermediate phases by XRD analysis. The X-ray powder diffraction pattern for these suboxides are presented in Figs. 2a and 2b. The XRD patterns of standards are included for comparison.

The development of the BET specific surface areas, S_g, of the intermediates is shown in Fig. 3. The S_g is seen to

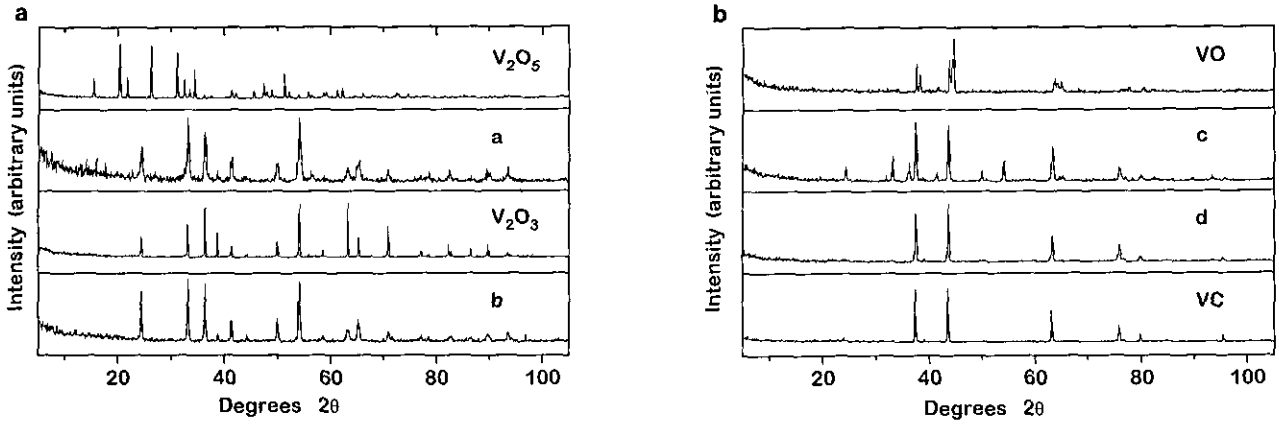

FIG. 2. (a) X-ray diffraction patterns of the intermediate phases *a* and *b* in VC synthesis and standard samples of V_2O_5 and V_2O_3. (b) X-ray diffraction patterns of the intermediate phases *c* and *d* in VC synthesis and standard samples of VO and VC.

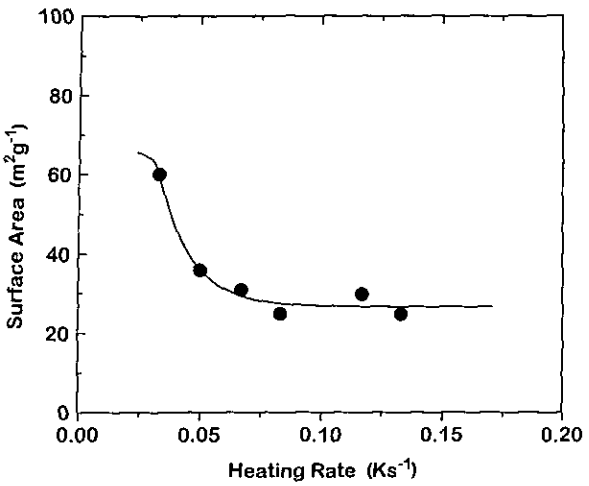

FIG. 4. The effect of heating rate on surface area of the final product.

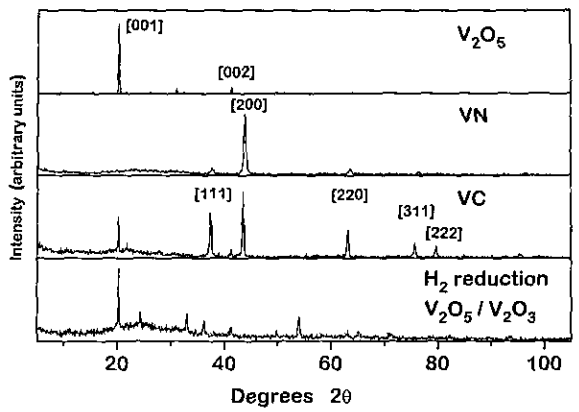

FIG. 5. X-ray diffraction pattern of preferentially oriented V_2O_5 and its nitrided, carburized, and reduced product.

increase from 19 $m^2 g^{-1}$ for V_2O_5 to 60 $m^2 g^{-1}$ for VC. The effect of heating rate, β, on S_g is shown in Fig. 4. Low heating rates are seen to produce higher surface areas, 60 $m^2 g^{-1}$ for $\beta = 0.03$ K s^{-1} while heating rates $\beta > 0.07$ give a product with $S_g \sim 30$ $m^2 g^{-1}$.

Table 1 provides the particle sizes, D_p, and the crystallite sizes, D_c. The particle sizes, D_p, were calculated from surface areas using the formula $D_p = 6/(S_g\rho)$ (9), where S_g is the specific surface area and ρ is the density. The crystallite sizes, D_c, were calculated from line broadening using the Scherrer equation (10), $D_c = K\lambda/B \cos\theta$, where $\lambda = 0.154$ nm, θ is the Bragg angle, B is the width of the XRD peak at half maximum corrected for instrumental broadening (0.1°), and K is a constant taken to be 0.9. The table also provides the lattice parameters for each of the intermediates. V_2O_3 has a corundum structure with lattice parameters $a_0 = 0.498$ and $c_0 = 1.388$ (11); VO and VC have rocksalt B1 cubic structures (space lattice, $Fm3m$). The lattice parameters, a_0, for $VO_{1.02}$ and $VC_{0.96}$ are 0.4077 and 0.4182 nm, respectively (11). Comparison of the above values with those in the table clearly identifies the cubic structure in intermediate c and d to be VC and not VO.

XRD patterns were used to determine topotacticity in the transformation. For a transformation to be topotactic, the crystallographic planes of the precursor should bear a spatial relationship to the final crystallographic planes of the product. Thus precursors with preferentially oriented planes should yield products that preserve the oriented crystalline structure. Figure 5 shows the XRD patterns of the VC obtained by carburizing V_2O_5 crystals that are preferentially oriented along {001} planes. The product phase, VC, is seen to have a pattern (Fig. 5) similar to the one derived from random V_2O_5 powders (intermediate d in Fig. 2b). The loss of the original oriented form indicates that the transformation is not topotactic. This is in contrast to the synthesis of VN using ammonia (Fig. 5) from the same precursor, which produced VN crystals oriented along {200} planes (8). The diffraction pattern of the oxide crystals reduced in pure H_2 is also given. In this case, the pattern shows the sample to contain a mixture of preferentially oriented V_2O_5 and randomly oriented V_2O_3.

TABLE 1

Compound	Phases	ρ (g cm^{-3})	D_p (nm)	D_c (nm)	Lattice parameters (nm) a_0	c_0
Precursor	V_2O_5	3.4	93	83	—	—
Intermediate *a*	V_2O_x	4.9	49	18	0.4941	1.3961
Intermediate *b*	V_2O_x		44	26	0.4952	1.3958
Intermediate c	V_2O_x			25	0.4950	1.3896
	VC	5.8	37		0.4155	—
Product *d*	VC		17	30	0.4160	—

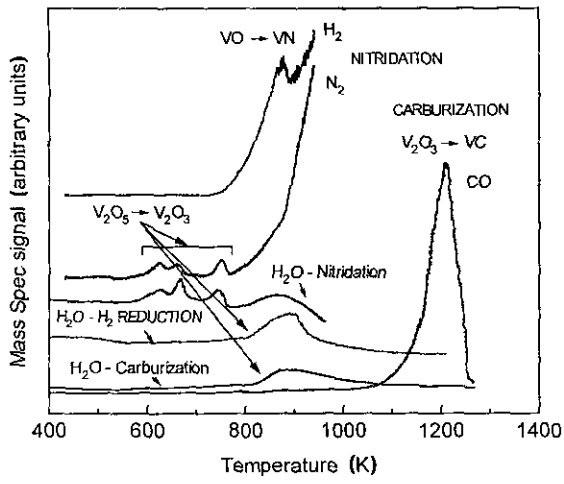

FIG. 6. Mass spectrometry signals for the TPR of V_2O_5; nitridation by 20% NH_3/He, reduction by 80% H_2/He, and carburization by 20% CH_4/H_2; β = 0.083 K s^{-1}.

DISCUSSION

The mass spectrometer trace (Fig. 1) shows that the vanadium carbide synthesis involves two reductive processes. In the first, the hydrogen component of the methane–hydrogen gas mixture reduces V_2O_5 to V_2O_3 with formation of H_2O around 700 K, and in the second, methane reduces and carburizes V_2O_3 to VC with formation of CO at higher temperatures.

$$V_2O_5 + 2H_2 \rightarrow V_2O_3 + 2H_2O \quad [1]$$

$$V_2O_3 + 5CH_4 \rightarrow 2VC + 3CO + 10H_2 \quad [2]$$

There is little surface area increase in the first stages, but there is a rapid increase in S_g after point c (Fig. 3). Thus, almost all of the increase in S_g takes place during the final reduction-carburization of V_2O_3 to VC. The abstraction of oxygen by CH_4 as CO as given by reaction [2] seems to be responsible for the increase in porosity and surface area. This presents an interesting contrast to the nitridation process (5), where there was a gradual increase in surface area at each intermediate phase formation. Also, in the case of nitrides (5), the $V_2O_5 \rightarrow V_2O_3$ transformation was not direct but involved suboxide phases of V_6O_{13}, V_2O_4, and VO_2. These were formed at lower temperatures (<800 K), gradually exposing surface area at each stage. In addition, the last stage $V_2O_3 \rightarrow$ VN, involved the suboxide VO before the formation of the nitride. Here, VO is not observed. Interestingly, the increase in surface area (~40 m^2 g^{-1}) during this second stage is the same for both carbides and nitrides. It is likely that the nitrides (90 m^2 g^{-1}) have higher surface areas than the carbides (60 m^2 g^{-1}) due to formation of the suboxides at lower temperatures. In the case of nitrides the reducing gas, NH_3, provides high concentrations of activated hydrogen species at lower temperatures than the carburizing gas mixture.

The combined TPR traces of V_2O_5 undergoing nitridation by ammonia, reduction by hydrogen, and carburization by a methane–hydrogen mixture, given in Fig. 6, offers a direct comparison of the different processes. The almost identical H_2O traces for the H_2 reduction and carburization experiments indicate that the active reducing species for the first stage is H_2. The figure also shows that for the same heating rate of β = 0.083 K s^{-1}, the final transformation temperature of the nitridation process (950 K) is considerably lower than that of the carburization process (1260 K). This is due to the stronger reducing and nitriding nature of ammonia. We have earlier shown that with ammonia

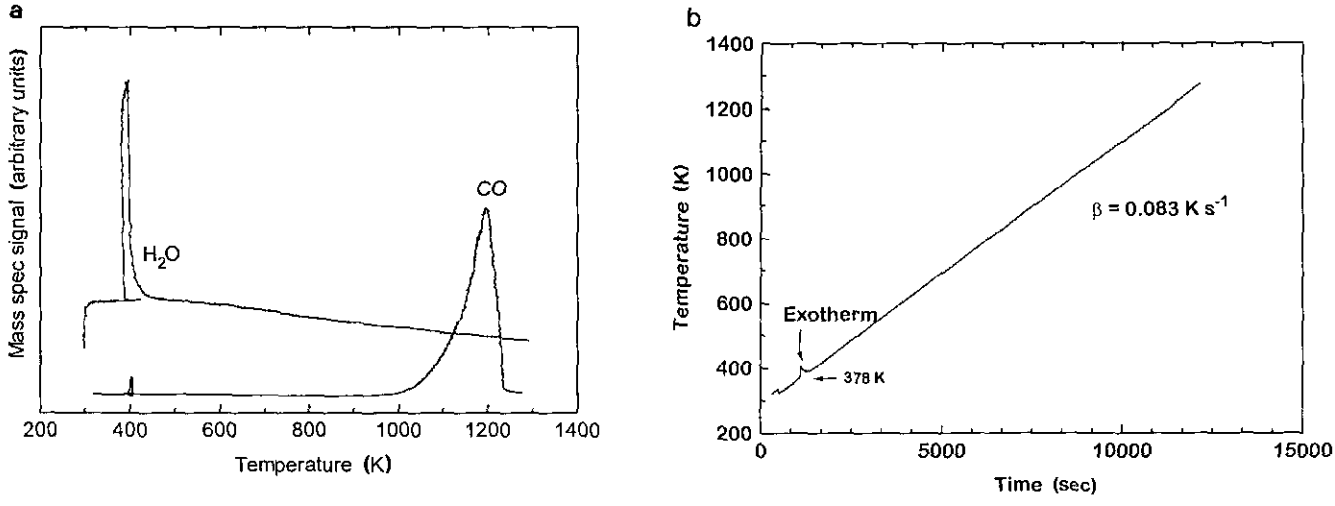

FIG. 7. (a) Mass spectrometry signal of H_2O and CO vs temperature, showing the progress of TPR of Pt/V_2O_5 with 20% CH_4/H_2; β = 0.083 K s^{-1}. (b) The plot of temperature program showing the exotherm at 378 K; β = 0.083 K s^{-1}.

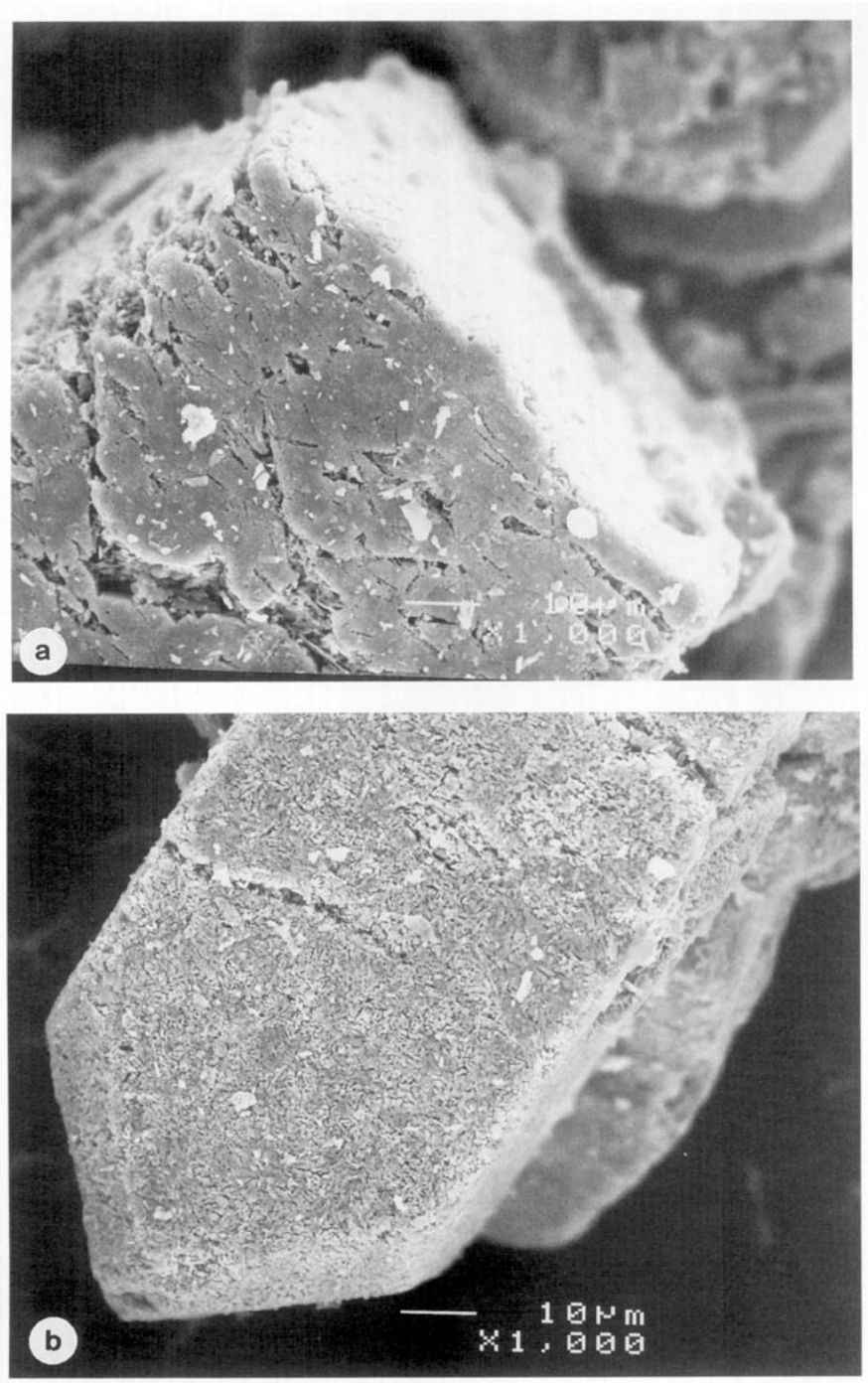

FIG. 8. SEM micrographs of (a) V_2O_5 × 1000, (b) VC × 1000, (c) V_2O_5 × 10,000, and (d) VC × 10,000.

the overall reductive process is limited by the diffusion of oxygen in the bulk (5). With hydrogen and methane the transformation is limited by the activation of these reactants on the surface of the vanadium oxide. This was demonstrated as follows.

Since noble metals are known to activate hydrogen easily, an experiment was carried out using 0.6% Pt/V_2O_5 as the precursor. Reduction of V_2O_5 by hydrogen assisted by Pt has been well studied in the past. It is believed that the platinum centers adsorb and dissociate molecular H_2 (12, 13), forming atoms which then migrate to reduce the oxide (hydrogen spillover).

The TPR trace for Pt/V_2O_5 under identical reaction conditions is given in Fig. 7a. The figure shows a very large H_2O peak at 390 K, and the characteristic CO peak at 1193 K. This shows that the noble metal, Pt, activates H_2

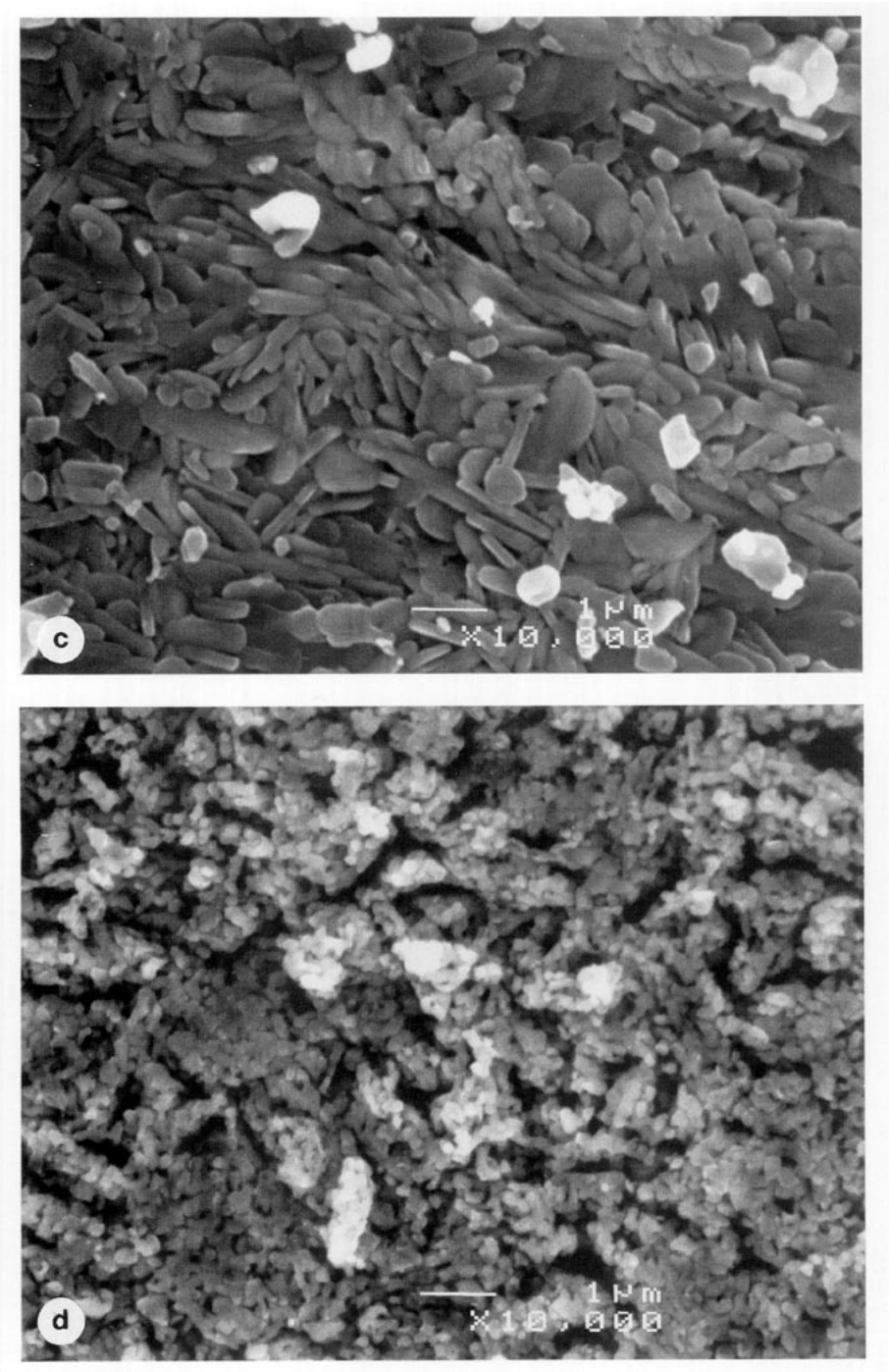

FIG. 8—*Continued*

at this low temperature initiating reduction of the oxide. The reduction is accompanied by an exotherm of 30 K at 378 K recorded by a thermocouple close to the bed (Fig. 7b). The exotherm is probably due to the heat of reaction ($V_2O_5 \xrightarrow{H_2} V_2O_3$, $\Delta H^\circ = -159$ kJ mol^{-1}). Theoretical calculations predict a local adiabatic temperature, ΔT_{ad}, rise of 710 K ($\Delta T_{ad} = \Delta H^\circ / C_p$, $C_p = 224$ J mol^{-1} K^{-1}). The local temperature probably shoots up to some high value, accelerating the reduction process. This explains the exotherm and the observed low peak temperature of 378 K.

At higher temperatures the hydrogen is not able to reduce V_2O_3 to VO as the process is not favored thermodynamically (standard free energy, $\Delta G^\circ > 0$) (14). It is not until higher temperatures (1260 K) that methane is activated so that the reduction of V_2O_3 occurs with the formation of CO. The transformation of V_2O_3 to VO becomes

thermodynamically feasible beyond 1230 K but at these temperatures the reaction cannot stop at the VO stage and the direct transformation to VC occurs (14).

In the TPR method there are two steps that can limit the overall synthesis of carbides and nitrides: oxygen diffusion and reactive gas activation. The first is a bulk process and the second is a surface process. Where the surface activation is fast, the synthesis will be limited by diffusion of oxygen (5) and will occur at the lowest possible temperature. This is the case for the reaction of vanadium oxide with the strong nitriding agent, ammonia, occurring a full 300 K lower than with the weak carburizing agent, methane (Fig. 6). Thus, by going to stronger carburizing agents like higher hydrocarbons, olefins, and acetylenes, it should be possible to lower the reaction temperature. This should also result in the occurrence of topotacticity. However, the substitution of methane by more reactive hydrocarbons could result in the deposition of surface carbon. The original choice of methane as a carburizing agent was based on thermodynamic calculations which predicted no free carbon formation (4).

In the experiment with preferentially oriented crystals, the XRD patterns (Fig. 5) show that the carbide loses the preferred orientation of the precursor and becomes randomly oriented. This clearly indicates that the transformation of $V_2O_3 \rightarrow VC$ is not topotactic. The same is also true for the reduction of $V_2O_5 \rightarrow V_2O_3$ by H_2. Here the pattern shows the final product to be a mixture of oriented V_2O_5 and random V_2O_3. In contrast, the transformation $V_2O_5 \rightarrow VN$ by ammonia is an example of a topotactic reaction (8).

Examination of the SEM micrographs (Figs. 8a and 8b) of the oxide and carbide shows the general retention of the shape and size of the macroscopic particles. Since density increases in the course of the transformation, the retention of external morphology is accompanied by the breakup of the crystallites making up the particles into smaller fragments (Figs. 8c and 8d) and consequently, an increase in surface area. The retention of external shape and size is called pseudomorphism and has been shown to also apply to VN synthesis (8). The occurrence of topotacticity in the case of VN but not VC formation is probably related to the temperatures of their transformations. Since VN is formed at relatively low temperatures where bulk diffusion is rate limiting, the solid-state transformation occurs with limited motions of atoms and structural relationships are retained. At higher temperatures dictated by surface reactions, as in the case of VC formation, diffusion is fast and structural features are erased. This is also the case in the molybdenum system. The transformation of MoO_3 to Mo_2N occurs at much lower temperatures than the transformation to Mo_2C and only the former is topotactic (15, 16).

Support by the U.S. Department of Energy, Grant DE-FG-22-95PC95207, is acknowledged.

CONCLUSION

Vanadium carbide synthesis involves a reduction of V_2O_5 to V_2O_3 by hydrogen around 800 K and a further reduction and carburization to VC by CH_4 with formation of CO around 1180 K. This is unlike VN synthesis where numerous intermediates were formed at lower temperatures. During the process, the surface area increased threefold with most of the increase occurring in the final stages of transformation. Heating rates of 0.03 K s^{-1} or less produce high surface areas. The carburization process was determined to be pseudomorphic but not topotactic. Activation of hydrogen using Pt/V_2O_5 did not change the final transformation temperature.

REFERENCES

1. G. W. Wilner and J. A. Berger, *J. Met.* **7,** 360 (1955); Y. M. Shy, L. E. Toth, and R. Somasundaram, *J. Appl. Phys.* **44,** 5539 (1973).
2. T. Yamada, M. Shimada, and M. Koizumi, *Ceram. Bull.* **59,** 611 (1980); R. Kieffer and F. Benesovsky, "Hartstoffe." Springer-Verlag, Vienna, 1963.
3. Following are reviews on synthesis and catalytic applications of transition metal carbides and nitrides: S. T. Oyama and G. L. Haller, "Catalysis Specialist Periodical Reports," (G. C. Bond and G. Webb, Eds.), Vol. 5, p. 333. Chem. Soc., London, 1981; S. T. Oyama, *Catal. Today* **15,** 179 (1992).
4. S. T. Oyama, J. C. Schlatter, J. E. Metcalfe, III, and J. M. Lambert, Jr., *Ind. Eng. Chem. Res.* **27,** 1639 (1988).
5. R. Kapoor and S. T. Oyama, *J. Solid State Chem.* **99,** 303 (1992).
6. R. Kapoor, Ph.D. Dissertation, Clarkson University, Potsdam, New York, 1994.
7. The gases employed in this study were a mixture of 20% CH_4/H_2 (Linde UHP Grade, 99.999), H_2 (Linde UHP Grade, 99.999%), and 0.5% O_2/He (Linde UHP Grade, 99.99%). The chemicals used were the vanadium oxides (described in the nitride study, Ref. 5), VC (Alfa, 99%), and $H_2PtCl_6 \cdot H_2O$ (Alfa, 99.9%). The latter was used to prepare 0.6% Pt/V_2O_5.
8. S. T. Oyama, R. Kapoor, H. T. Oyama, D. J. Hoffman, and E. Matijevic, *J. Mater. Res.* **8,** 1450 (1993).
9. J. M. Smith, "Chemical Engineering Kinetics" 3rd ed. McGraw–Hill, New York, 1981.
10. R. J. Matyi, L. H. Schwartz, and J. B. Butt, *Catal. Rev.-Sci. Eng.* **29,** 41 (1987).
11. Powder Diffraction Data File 31-1439, "Inorganic Phases." JCPDS International Center for Diffraction Data, Swathmore, PA, 1981.
12. N. I. Il'chenko, V. A. Lavrenko, V. L. Tikush, V. S. Zenkov, G. I. Golodets, and I. N. Frantsevich, *Dokl. Akad. Nauk SSSR* **218,** 1136 (1974).
13. N. I. Il'chenko, V. A. Yuza, and V. A. Roiter, *Dokl. Acad. Nauk SSSR* **172,** 133 (1967).
14. O. Knacke, O. Kubaschewski, and K. Hasselman, Eds., "Thermochemical Properties of Inorganic Substances" 2nd ed. Vols. I and II. Springer-Verlag, New York, 1991.
15. J. S. Lee, S. T. Oyama, and M. Boudart, *J. Catal.* **106,** 125 (1987).
16. L. Volpe and M. Boudart, *J. Solid State Chem.* **59,** 332 (1985).